

Electronic structure and magnetic properties of CrSb_2 and FeSb_2 investigated via ab-initio calculations

G. Kuhn, S. Mankovsky, and H. Ebert

*University of Munich, Department of Chemistry,
Butenandtstrasse 5-13, D-81377 Munich, Germany*

M. Regus and W. Bensch

*Institut für Anorganische Chemie, Christian-Albrechts-Universität zu Kiel,
Max-Eyth-Str. 2, D-24118 Kiel, Germany*

(Dated: November 5, 2018)

Abstract

The electronic structure and magnetic properties of CrSb_2 have been investigated by ab-initio calculations with an emphasis on the role of the magnetic structure for the ground state. The influence of correlation effects has been investigated by performing fixed spin moment (FSM) calculations showing their important role for the electronic and magnetic properties. The details of the electronic structure of CrSb_2 are analyzed by a comparison with those of FeSb_2 . The results obtained contribute in particular to the understanding of the temperature dependence of transport and magnetic behavior observed experimentally.

PACS numbers: Valid PACS appear here

I. INTRODUCTION

According to the experimental data available in the literature, the CrSb phase diagram shows two stable phases, having NiAs (CrSb) and marcasite (CrSb₂) structures [1–3], respectively. In the case of CrSb₂ with marcasite structure (space crystal group Pnmm) the Cr atoms are octahedrally coordinated by six nearest neighbor Sb atoms. As discussed in the literature, e.g. [4], CrSb₂ belongs together with FeSb₂ to the so-called 'Jahn-Teller' or 'regular' class of marcasites (characterized by a ratio of the lattice parameters $c/a \approx 0.53 - 0.57$, $c/b \approx 0.48$) in contrast to 'anomalous' marcasites (characterized by $c/a \approx 0.73 - 0.75$, $c/b \approx 0.62$)[4]. The 'regular' marcasites have an electronic structure leading to a Jahn-Teller instability with respect to octahedral symmetry, i.e. to a compression of the octahedral surrounding. This leads to a C_{2h} symmetry at the transition metal (TM) sites that gives rise to a corresponding splitting of the d -states in the crystal field [4, 5]. According to the element specific occupation of the splitted d -shell one can distinguish between the properties of low-spin $3d^4$ configuration occurring for FeSb₂ and high-spin $3d^2$ configuration of CrSb₂. Although the CrSb₂ and FeSb₂ compounds differ concerning these features, they have very similar crystal structures and therefore, it seems worth to consider them in parallel. In particular, is also motivated by the fact that only little information on CrSb₂ is available while the properties of FeSb₂ are investigated experimentally and theoretically in an extensive way [6–11]. From the literature it is known that FeSb₂ and CrSb₂ compounds are narrow-gap semiconductors at ambient pressure [1–3]. While FeSb₂ is nonmagnetic (NM) at low temperature, CrSb₂ has an antiferromagnetic (AFM) order with a magnetic moment of the Cr atom of about $1.94\mu_B$ [12, 13]. A temperature increase results in a transition from the small gap semiconductor to a metallic state with strong spin moment fluctuations [6]. This behavior is attributed to strong electron-electron correlation effects [6, 8–10, 14] that gives rise to the properties observed experimentally: the temperature dependence of magnetic susceptibility [8], the temperature dependent behavior of the electrical resistivity $\rho(T)$ [15, 16] and colossal thermopower $S(T)$ at $T = 10$ K [15, 16]. This behavior was found to be similar to that observed in FeSi with a Kondo insulator (KI) model as a possible scenario to describe the observed properties which have been investigated theoretically via LDA+U electronic structure calculations [17]. The corresponding investigations on FeSb₂ have been performed by Lukoyanov et al. [9] giving arguments for the KI description of the spin state

in FeSb₂. However, the origin of the electronic properties of FeSb₂ as well as of FeSi, is still under discussion. In particular the recent theoretical investigations [10, 14] gave arguments against the KI scenario of transition in these systems and discuss the effect of strong local dynamical correlations.

As was mentioned above, CrSb₂ has an AFM order below $T \approx 273$ K with a local magnetic moment of Cr atom of about $1.94\mu_B$ [12, 13]. The heat capacity observed in experiment has a lambda-shaped maximum at $T_N = 274.08$ K [18], which corresponds to a transition to the AFM state upon temperature decrease. The magnetic susceptibility $\chi(T)$ has an anomaly at $T = 55$ K which may be attributed [19] to a crossover between the different electronic states in the AFM semiconductor, but cannot be related to any magnetic transformation. No anomaly of the magnetic susceptibility has been observed near $T_N = 273$ K [19]. On the other hand, the electrical resistivity measurements show an anomaly at the Neel temperature 273 K, and at the same time has a plateau in the temperature regime 50–80 K. This finding is supposed to have a common origin with the susceptibility anomaly and is also attributed to a transition between the different semiconductive electronic states with the energy gap evaluated as $\Delta = 0.07$ eV. The behavior sketched for the resistivity has been observed by various experimental groups [13, 19–21]. In addition, Hu et al. [13] have demonstrated a rather pronounced anisotropy in the transport properties of FeSb₂ which is not observed in CrSb₂. The measurements of the transverse magnetoresistance (TM) $\frac{\rho(H) - \rho(0)}{\rho(0)}$ in a magnetic field up to $H = 90$ kOe at different temperatures exhibits an increase of this value with H^2 and then linearly as H increases further [19]. As has been pointed out [19], a similar behavior of the TM has been observed also for the FeSi semiconductor. The temperature dependent behavior of $\frac{\Delta\rho}{\rho(0)}$ exhibit a maximum at around $\approx 20K$.

Li et al. [21] have shown that the thermal conductivity of CrSb₂ has a maximum at $T \approx 50$ K, that they attributed to the effect of phonon-phonon Umklapp scattering. The thermopower S measured as a function of temperature is negative in the whole temperature range and has a large peak at ~ 60 K which correlates with the position of the plateau of the temperature dependent resistivity $\rho(T)$. For comparison, the thermopower $|S|$ in FeSb₂ has a giant maximum at $T \approx 10K$ and its thermal conductivity at ≈ 15 K. [15, 16]

A high-pressure experiment on CrSb₂ showed that for a pressure above 5.5 GPa a phase transition to the CuAl₂ structure occurs accompanied by ferromagnetic (FM) order with a Curie temperature $T \approx 160$ K and a saturation magnetic moment of about $1.2\mu_B$ per Cr

atom [22]. Experiments on FeSb₂ show no phase transitions up to 7 GPa [6]. This is in line with theoretical investigations that predict that for a transition from the marcasite to the CuAl₂ phase the pressure of about 41 GPa is required [23].

II. COMPUTATIONAL DETAILS

The calculation are done with the ELK code based on the FP-LAPW method [24]. To take into account correlation effects for Fe and Cr the calculations were done within the GGA as well as the GGA+U method. We used the exchange correlation functional by Perdew, Burke, Ernzerhof (PBE) [25]. For the GGA+U calculations the Coulomb (U) and exchange (J) parameters were chosen as follows: $U = 2.7$ eV and $J = 0.3$ eV for Cr and $U = 2.6$ eV and $J = 0.88$ eV for Fe [9]. As double counting correction the around mean field expression (AMF)[26–28] was used. The Cr magnetic moments presented below are calculated within the MT sphere with radius $R_{MT} = 2.32$ a.u. The experimental structure parameters used for CrSb₂ with marcasite structure are: $a = 6.1481$ Å, $b/a = 1.1404$, $c/a = 0.5428$ [29], and for FeSb₂: $a = 5.8328$ Å, $b/a = 1.1208$, $c/a = 0.5482$ [29].

III. RESULTS

Although there are several experimental results in the literature on CrSb₂, no detailed theoretical investigation have been done so far. Despite clear differences with FeSb₂, the two systems have also some common features. Therefore, it is interesting to analyze the properties of CrSb₂ in comparison with those of FeSb₂.

As a first step, electronic structure calculations for FeSb₂ and CrSb₂ have been performed based on the GGA using the experimental structure parameters. In the case of CrSb₂ with a small unit cell these calculations lead to a FM metallic ground state of the system (see the corresponding density of states (DOS) plot on the Cr atoms in Fig. 1c), in contradiction to the experimental results that show a small-gap semiconducting behavior for the system with AFM order. To describe the AFM order observed experimentally, supercell calculations are required, which will be discussed below. As a first step, we focus on the FM state of the system. In comparison, GGA calculations for FeSb₂ lead to a semiconducting NM state with the Fe DOS shown in Fig. 1a. GGA+U calculations performed to explain the

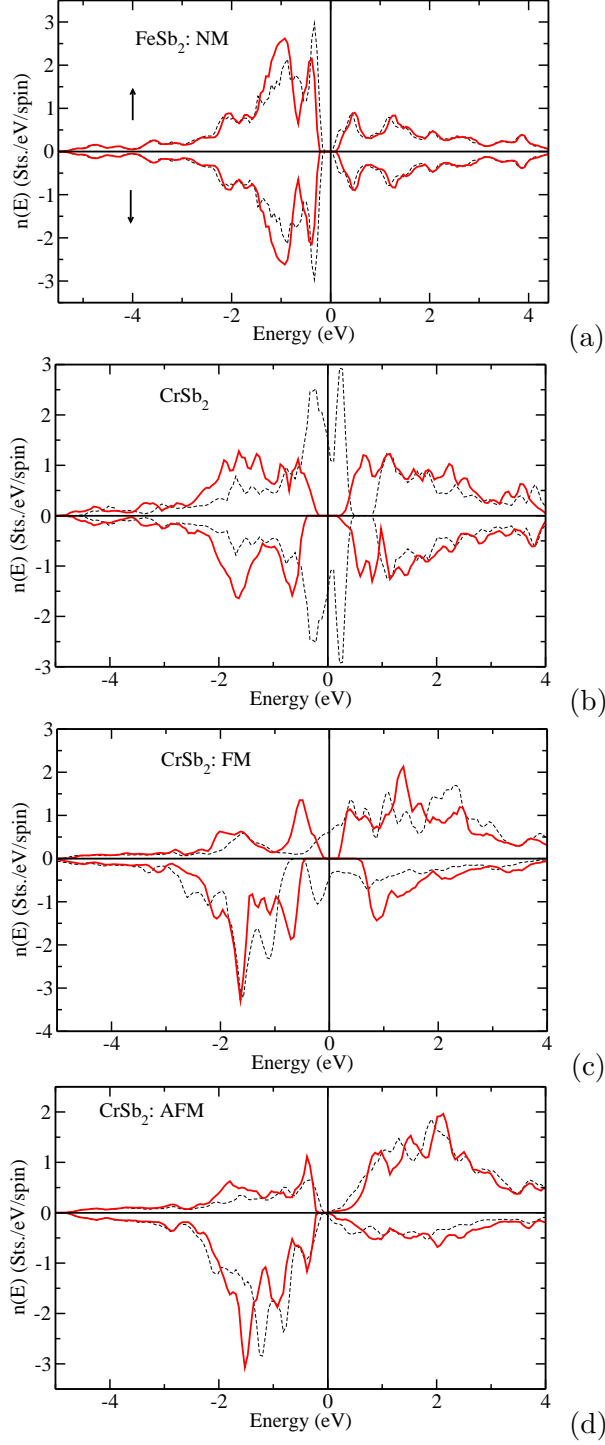


FIG. 1: Density of states on the transition-metal atoms in FeSb_2 (NM state) (a), and in CrSb_2 in NM (GGA results) and weakly magnetic with constrained magnetic moment $m_{Cr} = 0.05\mu_B$ (GGA+U results) (b), FM (c) and AFM (d) states. Solid and thin dashed lines represent the results of GGA+U ($U = 2.7$ eV for Cr and 2.6 eV for Fe) and GGA calculations, respectively.

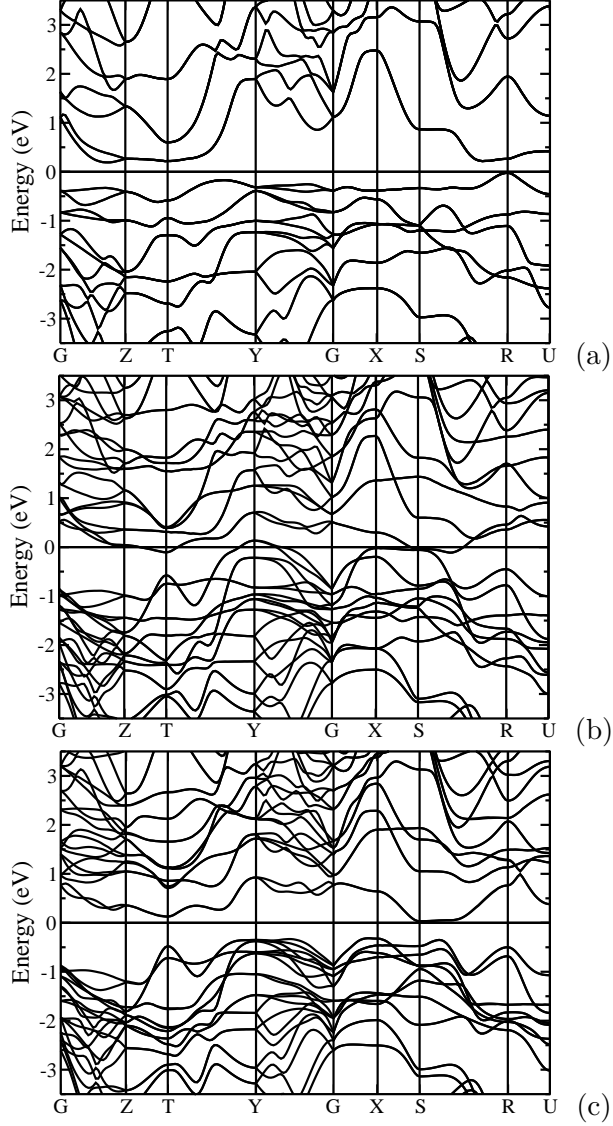


FIG. 2: Electronic band structure for NM FeSb₂ via GGA (a) and for FM CrSb₂ via GGA (b) and GGA+U, $U = 2.7$ eV (c)

finite temperature properties of FeSb₂ as reported in the literature demonstrate the crucial importance of a proper description of local correlations this compound. Motivated by this experience, GGA+U calculations have been performed also for CrSb₂.

To investigate the dependence of the results on the U parameter the calculations have been performed for different U value varying from 0 eV to 7 eV (see, e.g., the discussions in 17). In the following, if not otherwise noted, the results are presented for $U = 2.7$ eV as this value gives a well defined semiconducting state for CrSb₂ with FM order. However, it

should be noted, that in the case of AFM order, that is found experimentally [12, 13] for to the ground state, the U value does not play a crucial role for the semiconducting properties.

Fig. 1b displays the DOS on the Cr sites for NM CrSb₂ exhibiting metallic behaviour for GGA calculations (dashed line) with an energy gap above the Fermi level. Local correlations accounted for via GGA+U approach (with $U = 2.7$ eV) lead to a pronounced modification of the electronic structure even for a slightly spin-polarized system within LSM calculations with Cr magnetic moment of $0.05\mu_B$ (Fig. 1b, solid line). This results in a shift of the Fermi energy into the energy gap, i.e. the system becomes semiconducting.

In the case of CrSb₂ with FM order, selfconsistent GGA calculations (see the DOS in Fig. 1c) lead to a Cr magnetic moment of about $2.63\mu_B$ and a metallic state of the system. GGA+U results on the other hand exhibit the energy gap at the Fermi energy, different for the two different spin channels, and a magnetic moment of Cr atom of about $1.64\mu_B$. Corresponding modifications of the electronic structure can be seen in the energy band dispersion shown in Fig. 2, b (GGA) and c (GGA+U).

Calculations for the AFM state of CrSb₂ have been performed for the magnetic structure obtained experimentally [12]. Interestingly, in this case a small energy gap at the Fermi level occurs even within the GGA calculations. Local correlations treated via GGA+U only enhance the energy gap (see Fig. 1d) but do not result in further noteworthy modifications of the electronic structure.

Total energy calculations as a function of the volume have been performed for the NM, FM and AFM states of CrSb₂ with marcasite structure as well as for CrSb₂ in the FM state with CuAl₂ structure. The results are presented in Fig. 4. The volume in these calculations have been varied by a variation of the lattice parameter a , keeping the ratios b/a and c/a fixed as taken from experiment: $b/a = 1.1404$ and $c/a = 0.5428$ for marcasite structure [29], and $c/a = 0.885$ for CuAl₂ structure [22]. All calculations have been performed within the GGA+U ($U = 2.7$ eV) approach. Note that in the case of the CuAl₂ structure the difference in DOS results obtained via GGA and GGA+U is rather small and in both cases a metallic state of the system is observed (see Fig. 3).

From these calculations one can see that the AFM state for CrSb₂ with marcasite structure is indeed the ground state of the system as found in experiment, while the FM and NM states have slightly higher total energies. All total energy curves have a minimum at the volume which is nearly the same for different types of magnetic order and fits well to

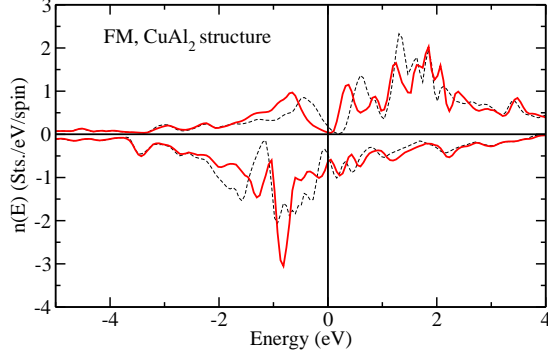


FIG. 3: Density of states on the Cr atoms for CrSb_2 with CuAl_2 structure in FM state. Solid and dashed lines represent the results of GGA+U ($U = 2.7$ eV) and GGA calculations, respectively.

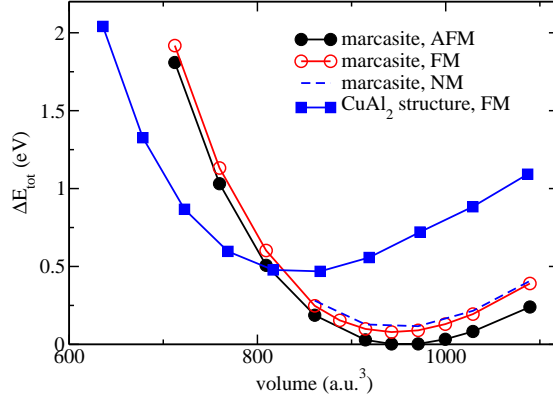


FIG. 4: Total energy of CrSb_2 calculated using the GGA+U for various magnetic phases with marcasite structure and for FM phase with CuAl_2 structure. The c/a and c/b ratios for all calculations have been kept constant at the experimental value [22, 29].

the experimental value. The curves for the marcasite structure have a crossing point with the curve for the CuAl_2 structure that has a minimum at a smaller volume than in the case of marcasite structure. These results are fully in line with the experimental data showing a transition from the marcasite to the FM CuAl_2 phase at the pressure of about 5.5 GPa [22].

The temperature dependence of transport and magnetic properties of CrSb_2 and the influence of correlation effects can be analyzed by performing fixed spin moment (FSM) calculations and comparing the results with the results for FeSb_2 . As was reported, e.g., by Lukoyanov et al. [9], the ground state of FeSb_2 is NM (see Fig. 5a). GGA+U calculations, on the other hand, result in an additional minimum at $1\mu_B$ (Fig. 5b) that is used to explain the strong spin fluctuations at high temperatures. According to the discussions by Lukoyanov

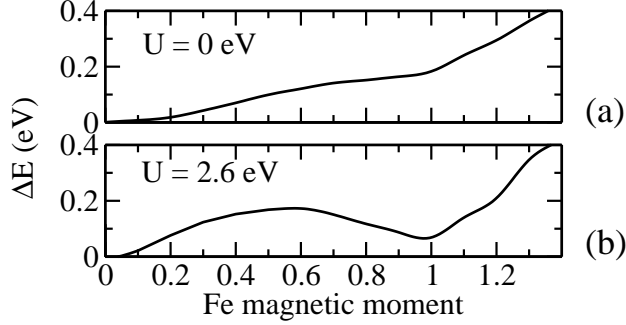


FIG. 5: The results of FSM calculations for FeSb₂: Total energy per unit cell vs fixed Fe magnetic moment via GGA (a) and GGA+U ($U = 2.6$ eV) (b).

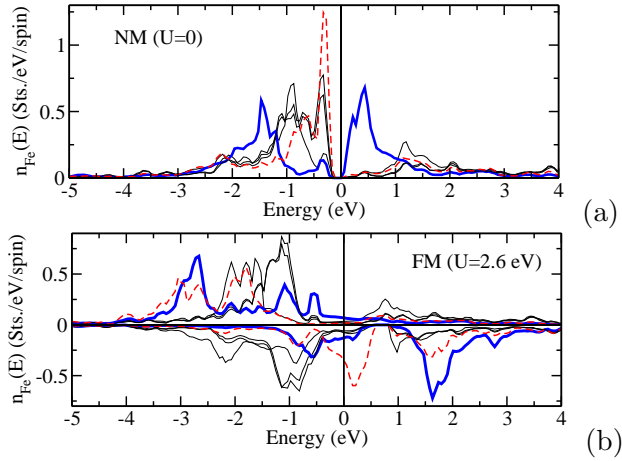


FIG. 6: Fe DOS in FeSb₂ obtained via GGA+U: for the NM (a, $U = 0$ eV) and FM (b, $U = 2.6$ eV) states. Thick solid line corresponds to $3d$ -states with d_{z^2} character, the dashed line shows the DOS of states with $d_{x^2-y^2}$ character.

et al. [9] on FeSb₂ as well as Anisimov et al. [17] on FeSi, this minimum is associated with the occupation of narrow Fe 3d-bands with d_{z^2} character at the bottom of the conduction band, and states of $d_{x^2-y^2}$ character near the top of the valence band (see Fig. 6). The results of corresponding FSM calculations for CrSb₂ are shown in Fig. 7. They exhibit rather different features when compared to FeSb₂. The GGA calculations show an absolute minimum for the total energy around a Cr magnetic moment of $2.0\mu_B$ (Fig. 7a), in contrast to FeSb₂ exhibiting a NM ground state. This means, the NM state of CrSb₂ (with the Cr DOS shown in Fig. 8a) is unstable with respect to the creation of a local magnetic moment on the Cr atoms. In general, this can lead either to FM or AFM order in the system with the corresponding Cr DOS shown in Fig. 8, b and d, respectively. This minimum is split into a

deeper at $\approx 1.8\mu_B$ and a more shallow one at $\approx 2.6\mu_B$ which depends essentially on the U value. The Cr DOS curves corresponding to these two minima are plotted in Fig. 9 a and b. One can see that the state with $\approx 1.8\mu_B$ is associated with the unoccupied majority-spin Cr $3d_{z^2}$ -states, while magnetic moment $\approx 2.6\mu_B$ is caused by additional occupation of Cr states of d_{z^2} character.

In the case of a higher magnetic moment the exchange splitting of the electronic states leads to an occupation of antibonding states in the spin-up channel and depleting of the bonding states in the spin-down channel. Such an occupation leads to a partial compensation of the energy gain due to the exchange splitting. Therefore, the FM state prefers to have an unoccupied $3d_{z^2}$ spin-up energy band, that is stabilized by treating local correlation effects via the GGA+U approach (see the DOS for $U = 2$ eV in Fig. 9 c and d). Thus, in the case of $U = 2$ eV the total energy within the FSM calculations has one minimum at $m = 0\mu_B$ and a second broad minimum in the regime 1.7 to $2.0\mu_B$. Fig. 9 c and d shows the DOS corresponding to the values of Cr magnetic moment $m = 1.7\mu_B$ and $m = 2.0\mu_B$. These results (for $U = 2$ eV, 2.7 eV) exhibit a similar behavior as in the case of FeSb₂ with the difference that the minimum at the finite magnetic moment is deeper. A further increase of the U value above 5 eV results in an instability of the FM state.

Another scenario is possible with a shift downwards in energy of the majority-spin $3d_{z^2}$ -states of Fe, changing their relative position with respect to the p states of Sb. This also leads to the arrangement of the Fermi level within the energy gap. This scenario is associated with an AFM state with the corresponding DOS shown in Fig. 8d (for $U = 0$) and Fig. 8e (for $U = 2.7$ eV). In this case GGA calculations result in a small-gap semiconducting state with a local Cr magnetic moment close to that obtained for the FM state (see Table 1), since Cr spin-up $3d_{z^2}$ -states in this case are also occupied. In contrast to FM case, the energy gap at E_F in this case occurs due to different spin-dependent hybridisation of the Cr d states with p states of Sb atoms. Also, in contrast to the FM state treated via GGA, AFM order in CrSb₂ is expected to be more stable since all bonding electronic states are occupied and antibonding states are not occupied. Altogether the GGA+U calculations result only in a slight variation of the electronic structure leading in particular to a decrease of the Cr magnetic moments.

From the results above one can draw the following conclusions. Stabilization of the AFM order as a ground state of CrSb₂ is related to a shift below the Fermi energy of Fe spin-up

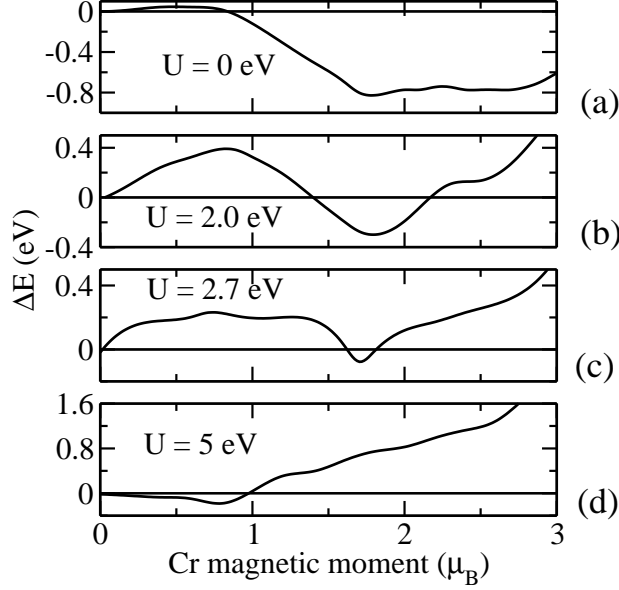


FIG. 7: The results of FSM calculations for CrSb₂ with FM order. Total energy per unit cell vs fixed Cr magnetic moment via GGA (a) and GGA+U: $U = 2$ eV (b), $U = 2.7$ eV (c), $U = 5.0$ eV (d).

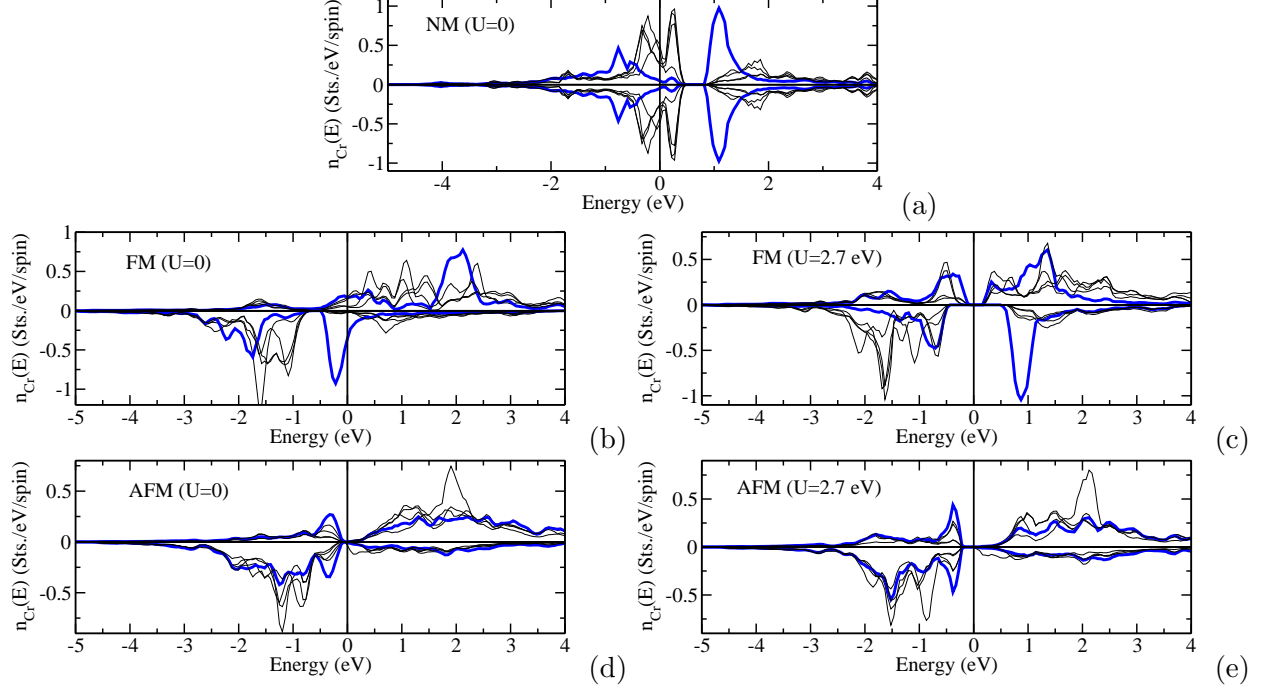


FIG. 8: Cr DOS for CrSb₂ in NM state (a, $U = 0.0$ eV), FM state (b, $U = 0.0$ eV) and (c, $U = 2.7$ eV), AFM state (d, $U = 0.0$ eV) and (e, $U = 2.7$ eV). Thick solid line corresponds to the $3d$ -states with d_{z^2} character.

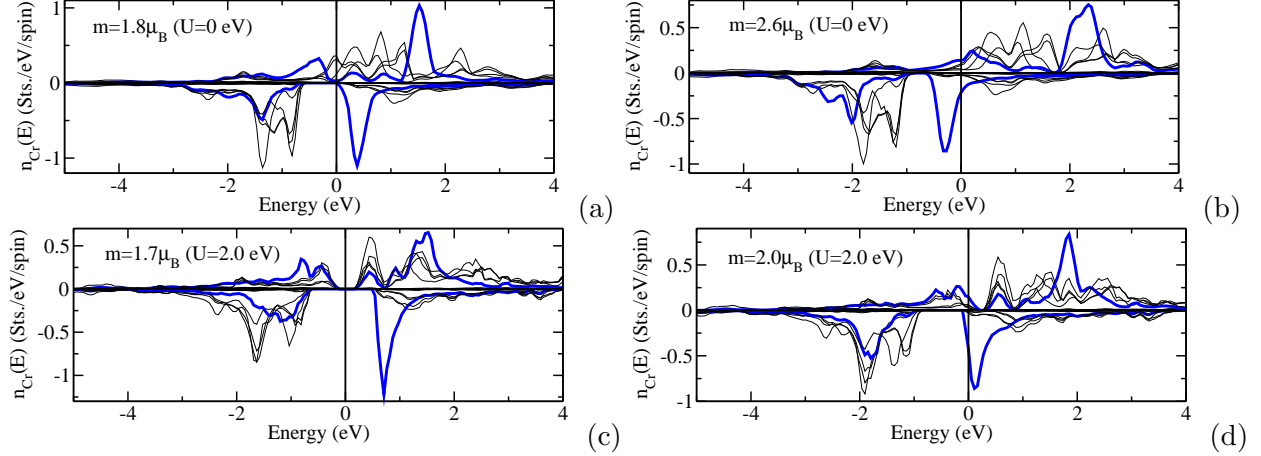


FIG. 9: Results of FSM calculations for CrSb_2 . Cr DOS in the FM state for the constrained Cr spin moment $m = 1.8\mu_B$ (a) and $m = 2.6\mu_B$ (b) for $U = 0.0$ eV); and $m = 1.7\mu_B$ (a) and $m = 2.0\mu_B$ (b) for $U = 2.0$ eV). Thick solid line corresponds to the $3d$ -states with d_{z^2} character.

states of d_{z^2} character with a corresponding modification of the spin-dependent hybridization of Cr d states and p states of Sb. This moves the Fermi level into the energy gap to make all bonding states to be occupied and antibonding states unoccupied. Local correlations treated via GGA+U influence in this case mainly the width of the energy gap. In the case of the metastable FM state GGA+U calculations lead to more crucial modifications of the electronic structure resulting in a semiconducting state of the system. This occurs due to a push up of the majority-spin d_{z^2} states of Cr above E_F in cost of stronger hybridization of minority-spin states with p states of Sb keeping the total number of electrons on the Fe atoms unchanged.

Although the FSM calculations have been performed only for the FM order, the results above allow also to expect that being in the AFM state, CrSb_2 should exhibit a metastable state determined by a different occupation of the d_{z^2} Cr states. Indeed, a temperature induced transition to the metastable state could explain the behavior of the susceptibility and transport properties observed experimentally at low temperature. It is possible that these two AFM states with slightly different electronic structure can be characterized also by different Cr local magnetic moments.

	GGA	GGA+U	Expt.
marcasite AFM	2.57	2.03	1.94
marcasite FM	2.62	1.64	-
CuAl ₂	2.23	1.97	1.2

FIG. 10: Magnetic moments in μ_{Bohr} per atom for CrSb₂ (in the MT sphere with radius $R_{MT} = 2.32$ a.u.) within the GGA and GGA+U calculations. Theoretical results are compared with experimental data. [12, 22]

IV. CONCLUSION

In summary, one has to stress that the AFM order in CrSb₂ plays a crucial role for the type of conductivity in the system exhibiting the small-gap semiconducting properties. Although the local correlations treated via the GGA+U approach influence mainly the width of the energy gap of CrSb₂, their role can be important to describe the experimental results as it was shown for FeSb₂. In general, the present theoretical results are in a good agreement with the experiment, showing the AFM ground state of CrSb₂ with marcasite structure, with a Cr local magnetic moment of about $2.03\mu_B$ and with a small energy gap at the Fermi level. Concluding from the total energy calculations a phase transition under pressure to the CuAl₂ phase exhibiting the properties of FM metal should be observed.

Acknowledgments

Financial support by the *Deutsche Forschungsgemeinschaft* within the framework of the priority program (*DFG-Schwerpunktprogramm 1415*) *Kristalline Nichtgleichgewichtsphasen (KNG) - Präparation, Charakterisierung und in situ-Untersuchung der Bildungsmechanismen* is gratefully acknowledged.

[1] A. Holseth, Hans; Kjekshus, Acta Chemica Scandinavica **22**, 3273 (1968), URL <http://actachemscand.dk/volume.php?select1=3&vol=22>.

- [2] A. A. A. F. Holseth, Hans; Kjekshus, *Acta Chemica Scandinavica* **24**, 3309 (1970), URL <http://actachemscand.dk/volume.php?select1=4&vol=24>.
- [3] A. Brostigen, Gunnar; Kjekshus, *Acta Chemica Scandinavica* **24**, 2983 (1970), URL <http://actachemscand.dk/volume.php?select1=4&vol=24>.
- [4] F. Hulliger and E. Mooser, *J. Phys. Chem. Sol.* **26**, 429 (1965), ISSN 0022-3697, URL <http://www.sciencedirect.com/science/article/pii/0022369765901733>.
- [5] J. B. Goodenough, *J. Solid State Chem.* **5**, 144 (1972), ISSN 0022-4596, URL <http://www.sciencedirect.com/science/article/pii/0022459672900229>.
- [6] C. Petrovic, Y. Lee, T. Vogt, N. D. Lazarov, S. L. Bud'ko, and P. C. Canfield, *Phys. Rev. B* **72**, 045103 (2005), URL <http://link.aps.org/doi/10.1103/PhysRevB.72.045103>.
- [7] I. A. Zaliznyak, A. T. Savici, V. O. Garlea, R. Hu, and C. Petrovic, *Phys. Rev. B* **83**, 184414 (2011), URL <http://link.aps.org/doi/10.1103/PhysRevB.83.184414>.
- [8] P. Sun, M. Sndergaard, B. Iversen, and F. Steglich, *Ann. Physik* **523**, 612 (2011), ISSN 1521-3889, URL <http://dx.doi.org/10.1002/andp.201100033>.
- [9] A. V. Lukoyanov, V. V. Mazurenko, V. I. Anisimov, M. Sigrist, and T. M. Rice, *Eur. Phys. J. B* **53**, 205 (2006), ISSN 1434-6028, 10.1140/epjb/e2006-00361-0, URL <http://dx.doi.org/10.1140/epjb/e2006-00361-0>.
- [10] J. Kuneš and V. I. Anisimov, *Phys. Rev. B* **78**, 033109 (2008), URL <http://link.aps.org/doi/10.1103/PhysRevB.78.033109>.
- [11] R. Miao, G. Huang, C. Fan, Z. Bai, Y. Li, L. Wang, L. Chen, W. Song, and Q. Xu, *Solid State Commun.* **152**, 231 (2012), ISSN 0038-1098, URL <http://www.sciencedirect.com/science/article/pii/S003810981100559X>.
- [12] A. A. A. F. Holseth, Hans; Kjekshus, *Acta Chemica Scandinavica* **24**, 3309 (1970), URL <http://actachemscand.dk/volume.php?select1=4&vol=24>.
- [13] R. Hu, V. F. Mitrović, and C. Petrovic, *Phys. Rev. B* **76**, 115105 (2007), URL <http://link.aps.org/doi/10.1103/PhysRevB.76.115105>.
- [14] V. V. Mazurenko, A. O. Shorikov, A. V. Lukoyanov, K. Kharlov, E. Gorelov, A. I. Lichtenstein, and V. I. Anisimov, *Phys. Rev. B* **81**, 125131 (2010), URL <http://link.aps.org/doi/10.1103/PhysRevB.81.125131>.
- [15] A. Bentien, S. Johnsen, G. K. H. Madsen, B. B. Iversen, and F. Steglich, *Europhys. Lett.* **80**, 17008 (2007), URL <http://stacks.iop.org/0295-5075/80/i=1/a=17008>.

- [16] P. Sun, N. Oeschler, S. Johnsen, B. B. Iversen, and F. Steglich, *Phys. Rev. B* **79**, 153308 (2009), URL <http://link.aps.org/doi/10.1103/PhysRevB.79.153308>.
- [17] V. I. Anisimov, S. Y. Ezhov, I. S. Elfimov, I. V. Solovyev, and T. M. Rice, *Phys. Rev. Lett.* **76**, 1735 (1996), URL <http://link.aps.org/doi/10.1103/PhysRevLett.76.1735>.
- [18] A. Alles, B. Falk, E. F. W. Jr., and F. Grnvold, *The Journal of Chemical Thermodynamics* **10**, 103 (1978), ISSN 0021-9614, URL <http://www.sciencedirect.com/science/article/pii/0021961478901167>.
- [19] Y. Takahashi, T. Harada, T. Kanomata, K. Koyama, H. Yoshida, T. Kaneko, M. Motokawa, and M. Kataoka, *J. Alloys Comp.* **459**, 78 (2008), ISSN 0925-8388, URL <http://www.sciencedirect.com/science/article/pii/S0925838807012121>.
- [20] T. Harada, T. Kanomata, Y. Takahashi, O. Nashima, H. Yoshida, and T. Kaneko, *J. Alloys Comp.* **383**, 200 (2004), ISSN 0925-8388, *Proceedings of the 14th International Conference on Solid Compounds of Transition Elements (SCTE 2003)*, URL <http://www.sciencedirect.com/science/article/pii/S0925838804004827>.
- [21] H. Li, X. Qin, D. Li, and H. Xin, *J. Alloys Comp.* **472**, 400 (2009), ISSN 0925-8388, URL <http://www.sciencedirect.com/science/article/pii/S0925838808007135>.
- [22] H. Takizawa, K. Uheda, and T. Endo, *J. Alloys Comp.* **287**, 145 (1999), ISSN 0925-8388, URL <http://www.sciencedirect.com/science/article/pii/S0925838899000560>.
- [23] X. Wu, G. Steinle-Neumann, S. Qin, M. Kanzaki, and L. Dubrovinsky, *J. Phys.: Cond. Mat.* **21**, 185403 (2009), URL <http://stacks.iop.org/0953-8984/21/i=18/a=185403>.
- [24]
- [25] J. P. Perdew, K. Burke, and M. Ernzerhof, *Phys. Rev. Lett.* **77**, 3865 (1996), URL <http://link.aps.org/doi/10.1103/PhysRevLett.77.3865>.
- [26] A. Liechtenstein, V. Anisimov, and J. Zaanen, *Phys. Rev. B* **52**, R5467 (1995), URL http://prb.aps.org/abstract/PRB/v52/i8/pR5467_1.
- [27] F. Bultmark, F. Cricchio, O. Grånäs, and L. Nordström, *Phys. Rev. B* **80**, 035121 (2009), URL <http://link.aps.org/doi/10.1103/PhysRevB.80.035121>.
- [28] M. T. Czyżyk and G. A. Sawatzky, *Phys. Rev. B* **49**, 14211 (1994), URL <http://link.aps.org/doi/10.1103/PhysRevB.49.14211>.
- [29] A. Holseth, Hans; Kjekshus, *Acta Chemica Scandinavica* **22**, 3284 (1968), URL <http://actachemscand.dk/volume.php?select1=3&vol=22>.